

# 5

---

## Smartphone-Based Photoplethysmogram Measurement

---

Yuriy Kurylyak, Francesco Lamonaca and Domenico Grimaldi

*Department of Electronics, Computer and System Sciences, University of Calabria,  
Rende – CS, Italy; e-mail: {kurylyak, flamonaca, grimaldi}@dets.unical.it*

### Abstract

Smartphones have become one of the widest and often used devices that people bring almost every time and everywhere. Their computational capacities allow their application to many every-day tasks. One of them is health state monitoring. This chapter presents a smartphone-based photoplethysmogram (PPG) acquisition and pulse rate evaluation system. The proposal was designed for different smartphone models, equipped with a LED or not. Different cameras represent the same acquired information in different ways: changes may occur in color saturation, resolution, frame rate, etc. Therefore, several smartphones were used to define the common characteristics of the captured video, and establish proper criteria for PPG extraction. Moreover, the appropriate algorithms were proposed and validated to verify the correct device usage, the system calibration, the PPG and pulse rate evaluation. The experimental results have confirmed the correctness and suitability of the proposed method with respect to the medical pulse measurement instruments.

**Keywords:** photoplethysmography, pulse wave analysis, pulse rate measurement, smartphone, non-invasive monitoring.

## 5.1 Introduction

Monitoring of vital parameters is very important for timely detection and prevention of any health diseases. The blood pressure, heart rate and their changes are ones of the most important parameters to control.

There are different techniques to control heart activity: electrocardiography, ambulatory blood pressure monitoring, photoplethysmography, etc. When patients are asked to measure their own heart rate, usually the palpation technique is used, however it is not precise. Therefore, individuals should be properly trained on how to measure their own heart rate accurately [1]. To overcome the human factor automatic systems have been proposed.

### 5.1.1 Electrocardiography

Electrocardiography (ECG) allows evaluating the performance of the cardiovascular system with high accuracy, and it is “a gold standard” for beat-to-beat heart rate (HR) measurements [2]. It is an interpretation of the electrical activity of the heart, detected by the electrodes attached to the skin, and recorded by an ECG machine over a time interval [3]. Each heart beat is represented by a regular sequence of wave patterns (Figure 5.1).

However, the ECG requires attaching and correctly placing multiple electrodes on the body. That limits the device usage to a clinical environment with trained personnel and makes such approach impractical for most individuals interested in monitoring their HR in natural environments [2].

Moreover, many patients are subjects to a so-called “white coat effect”. In particular, several studies of white coat effect have confirmed that it occurs in 20% or more of the hypertensive population [4]. The white coat hypertension is defined as the presence of increased blood pressure due to nervousness when undergoing a clinical examination, while at home it remains normal. Indeed, according to a recent research by Kaiser Permanente Colorado in collaboration with the American Heart Association and Microsoft Corp., patients performing self-monitoring of their vital parameters are 50% more likely to



Figure 5.1 ECG wave with detected heart beats.

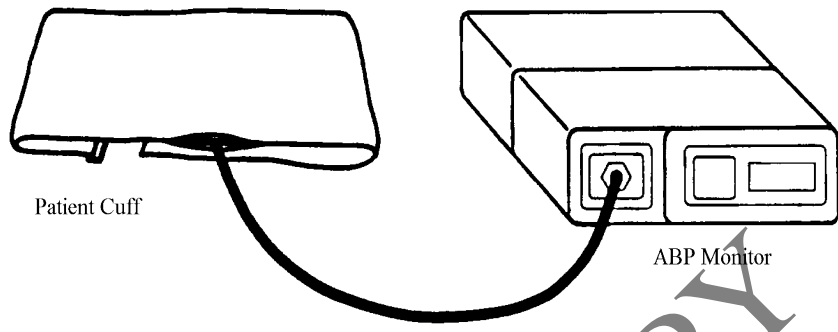


Figure 5.2 Spacelabs 90207 ABP Monitor.

have their blood pressure under control [5]. Therefore, there is a need for low-cost physiological monitoring solutions that are easy to use, accurate, and can be used at home or in ambulatory conditions [6].

There are alternative portable ECG devices such as Holter monitors that allow continuous monitoring of the cardiovascular system. Once the electrodes are attached to the chest, the patient can continue normal activities for 24 hours or more. Then, the cardiologist analyzes the recorded ECG and diagnoses. The main drawback of such solution is that there is no immediate feedback to the user, so there is no possibility to help the patient when the incident occurs [7].

### 5.1.2 Ambulatory Blood Pressure Monitoring

In a similar way, Ambulatory Blood Pressure (ABP) monitoring devices are used for non-invasive examination of heart activity. They provide continuous 24 hour measurements of the blood pressure and HR at regular time intervals. Having been developed mostly to identify patients with white coat hypertension, they become very useful for the determination of hypertensive end-organ damage risk [8]. For example, a Spacelabs 90207 ABP Monitor (Figure 5.2) [9] is a clinically validated medical device [10–12] tested according to the protocols of the Association for the Advancement of Medical Instruments [13], the American Heart Association [14], and the British Hypertension Society [15].

However, as in the case of portable ECG devices, the ABP monitoring devices are expensive and do not provide the real time measurement results. Patients should visit their doctors for viewing and analyzing the measurements.

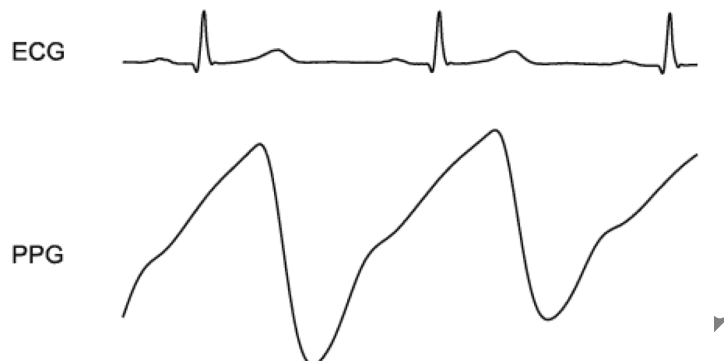


Figure 5.3 The pulsatile (AC) component of the PPG signal and the corresponding electrocardiogram [16].

### 5.1.3 Photoplethysmography

An alternative non-invasive technique for the detection of blood volume changes during a cardiac cycle is photoplethysmography (PPG). It is a simple and low-cost optical technique that can be used to detect blood volume changes in the microvascular bed of tissue [16]. The technique assumes skin illumination with penetrating optical radiation, usually from a light emitting diode, with a subsequent detection of the signal by a photodetector [17]. Most often the PPG operates at a red or a near infrared wavelength [16].

The PPG has considerable potential for telemedicine including home/remote patient health monitoring. Miniaturization, ease-of-use and robustness are key design requirements for such systems [16]. Clinical PPG applications include monitoring of heart and respiration rate, blood oxygen saturation, pressure as well as detection of peripheral vascular diseases [17].

The PPG waveform consists of a pulsatile (“AC”) physiological waveform attributed to cardiac synchronous changes in the blood volume, and a slowly varying (“DC”) baseline. The “AC” component has its fundamental frequency typically around 1 Hz, depending on the heart rate. The “DC” component is influenced by respiration, sympathetic nervous system activity and thermoregulation [16]. Figure 5.3 shows the pulsatile component of an acquired PPG waveform and the corresponding electrocardiogram.

As was mentioned, the “AC” component corresponds to the heart beats and can be used for heart activity monitoring. The PPG probe should be held securely in place to minimize the probe-tissue movement artifacts [16].

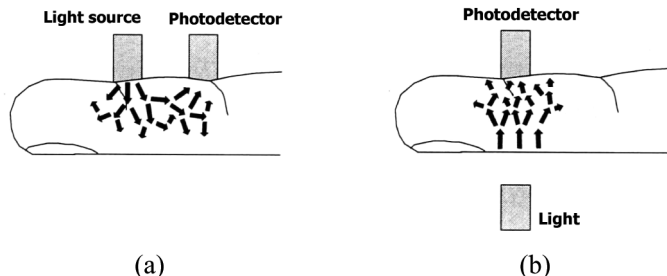


Figure 5.4 Reflection (a), and transmission (b) modes for video acquisition [18].



Figure 5.5 CMS50DL finger pulse oximeter SpO<sub>2</sub> monitor.

There are two possible PPG operational modes: (1) transmission, when the tissue sample (e.g. fingertip) is placed between the source and detector (Figure 5.4a), and (2) reflection when the LED is placed next to the detector (Figure 5.4b) [18]. The transmission mode imposes more restrictions than the reflection mode on the body locations available for study [16].

Such photometric-based plethysmogram is normally obtained by using a pulse oximeter (Figure 5.5) [19, 20]. The device is placed on a thin part of the subject's body, usually a fingertip or earlobe. The light with red and infrared wavelengths sequentially passes through the subject to a photo-detector that measures the changes in light absorption [21].

In addition to the PPG waveform, an oximeter evaluates the level of oxygen in blood and computes a pulse rate (PR). Figure 5.6 shows typical information obtained by the CMS50DL oximeter and displayed by the SpO<sub>2</sub> software, which comes with the device.

The PPG signal obtained in this way is familiar to clinicians [20]. It clearly shows the pulsatile waveform caused by the pressure wave from the cardiac cycle, and the respiratory sinus arrhythmia induced by breathing [21].

Since the pulse oximeter is non-invasive and relatively inexpensive, in addition to the PR and level of oxygen in blood provided by such devices, much

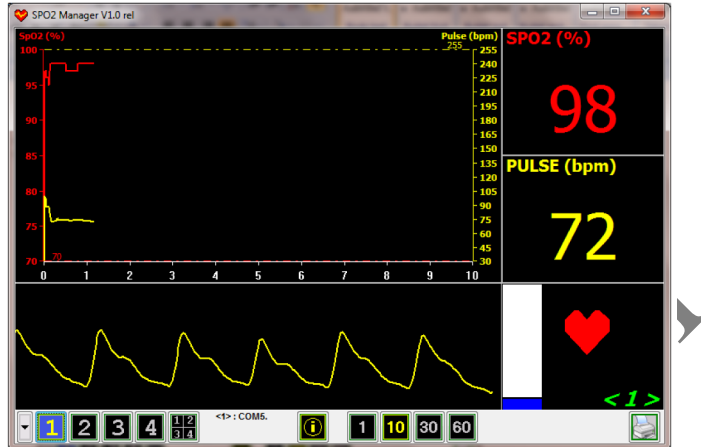


Figure 5.6 Measurement results showed in SpO2 Manager.

research has been carried out in extracting additional biometric information from the waveform. Linder et al. [21] extracted the following parameters from the obtained PPG: the pulse height, peak threshold, cardiac period, full width half max, and peak width (Figure 5.7), and used it to detect changes in posture.

Analysis of the blood volume pulse contour has become important because it contains much information about cardiovascular activity [22]. The final goal is to use the pulse oximeter as a primary sensor in an affordable, wearable health monitoring system [21].

#### 5.1.4 Photoplethysmography Imaging

Replacing the photodetector, used in pulse oximeters, by a video camera enables photoplethysmography imaging. It is an emerging area for research that provides advantages in terms of improved sensitivity, and real-time large surface area measurement [23]. Optical video monitoring of the skin by a digital camera provides information related to the subtle color changes caused by the cardiac signal, and the pulsatile signal [6].

A preliminary CCD camera-based imaging photoplethysmographic system was described in [23, 24]. Fast digital cameras allow the development of PPG imaging, a totally contactless technique for monitoring a larger field of view and different depths of tissue by applying multi-wavelength LEDs. The PPG imaging system can work in both transmission and reflection modes as

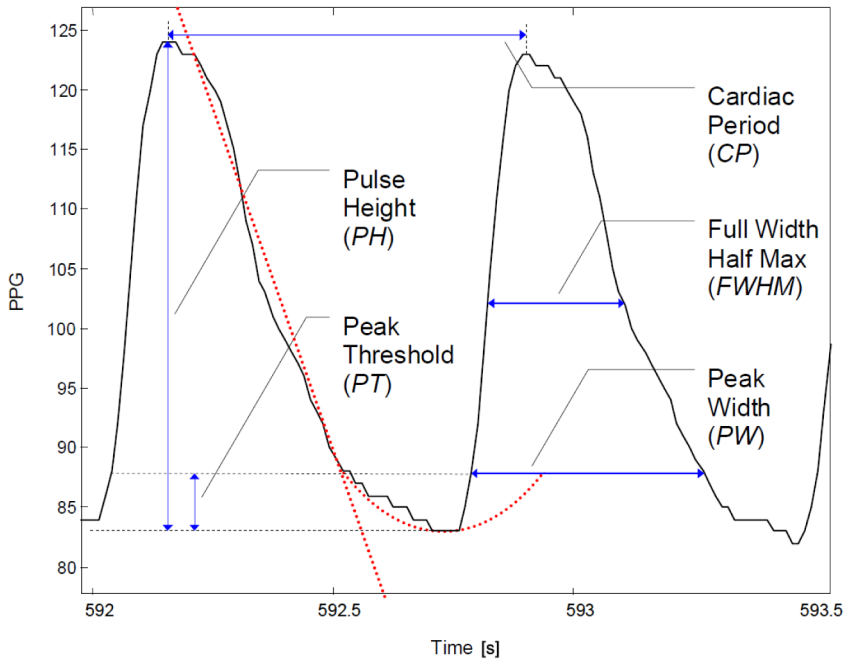


Figure 5.7 The features of the PPG pulsatile component used in [21]: Pulse Height, Peak Threshold, Cardiac Period, Full Width Half Max, and Peak Width.

it is depicted in Figure 5.8. The light intensity that passes through the finger varies with the pulsing of the blood and its plot against time is referred to a PPG signal.

### 5.1.5 Smartphone-based Health Monitoring Systems

Nowadays smartphones have become one of the widest and often used devices that people bring almost everywhere. In addition, their computational power, possibility of wireless communication as well as their multifunctional user interface allows their usage in very wide spheres.

Smartphones are often used in telemonitoring to receive information from portable medical devices (e.g., blood pressure, glucose and pulse oximeter monitors) and mobile sensors (e.g., physical activity, accelerometer counts, heart rate, respiration rate, pulse pressure, and wireless electrodes) [2]. As an example, the iHealth Lab Inc. has announced the iHealth Blood Pressure Monitoring System for the iPhone, iPod Touch and iPad (Figure 5.9) [25].

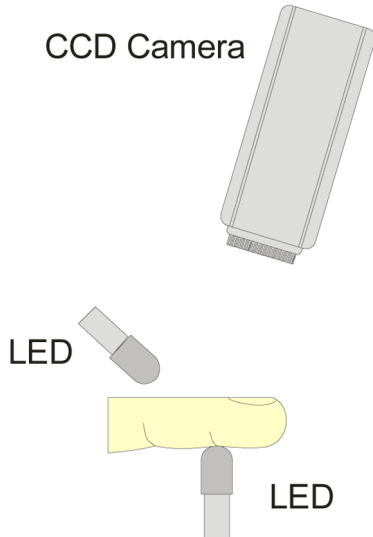


Figure 5.8 Signal acquisition principle of a PPG imaging system.



Figure 5.9 The iHealth Blood Pressure Monitoring System.

It consists of a hardware dock, a blood pressure arm cuff and software, and allows the users to self-monitor their blood pressure at home as well as share results with a doctor. There are also pulse oximeters capable of sending the measured results to smartphones using Bluetooth or Wi-Fi connection.

Such devices can be organized then into personalized health monitoring systems (Figure 5.10). The patient fixes sensors (e.g. oximeter) on the

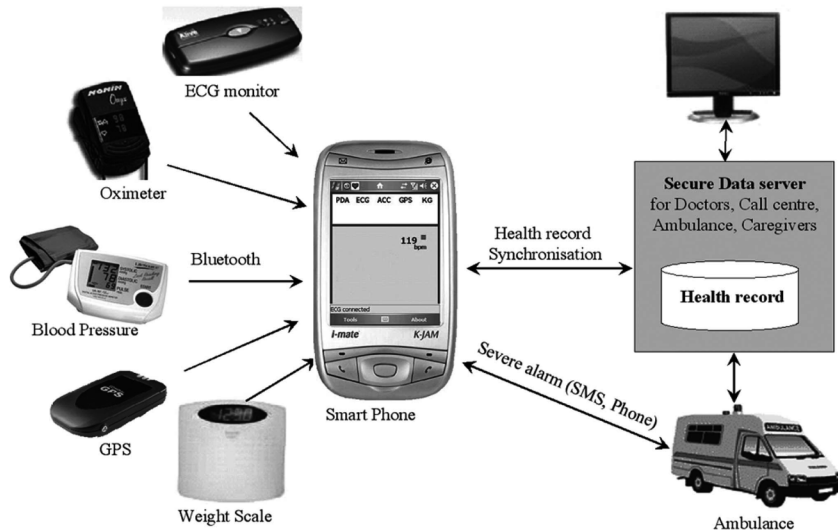


Figure 5.10 Personalized health monitoring architecture [7].

body that communicate with a smartphone sending measurement results. The smartphone then processes the received data and monitors the patient's health. In the case of emergency, it automatically calls an ambulance or sends an SMS to the doctor with the location of the patient and the reason [7, 26].

There are different health and healthcare smartphone applications already available on the market for Android, Apple iOS, RIM BlackBerry, Symbian, Windows Mobile 6.x and Windows Phone 7. As an example we can cite an EU-funded project for older people with multiple chronic conditions eCAALYX (Enhanced Complete Ambient Assisted Living Experiment). The smartphone-based application receives data from the patient-wearable wireless health sensors and communicates over the Internet with a remote server accessible by healthcare professionals who are in charge of the remote monitoring and management of the older patient with multiple chronic conditions [27].

### 5.1.6 Smartphone-based Photoplethysmography

Most of the current generation cellular phones are equipped with high-resolution cameras, processors and light-emitting diode flashes (LEDs). This is very similar to the PPG imaging technology and, therefore, instead of using a smartphone just as a device for storing and visualizing measured data, they

can directly measure some vital characteristics. Smartphones can be used for the express-measurement of such vital characteristics as pulse rate [2, 6, 17, 28], breathing rate [29], as well as providing deeper analysis of the PPG waveform in order to extract additional data [30].

Nowadays, there are smartphone-based commercial applications such as Instant Heart Rate, Heart Rate Tester, Pulse Rate Monitor, Cardiograph, etc. that allow evaluating HR. However, while they provide a PPG-like waveform in the ideal usage conditions, they often fail when something goes wrong. Moreover, there is no comparison to the medical devices and, as reported by developers, such applications should be used for reference only but not as a medical tool.

Pelegris et al. proposed a novel method to detect heart beat rate using a mobile phone [28]. In particular, they proposed to analyze brightness information of the grayscale portion of every captured frame, while the user keeps his/her finger on the lens. To ensure reliability of acquisition, the input signal is matched to a crude heart beat pattern of alternating peaks and troughs. The results were based on the Nokia N95 smartphone, and the authors reported a performance problem of the Android-based smartphone.

Jonathan and Leahy used a Nokia E63 smartphone for pulse rate measurement, and they assessed that the green channel provides a stronger PPG signal than the red one [17, 31]. A central region of interest measuring  $10 \times 10$  pixels was selected in order to compute the mean intensity value, and a Fourier transform spectral analyses was applied to evaluate the heart rate. The authors reported a possibility to detect changes in HR from rest to after exercise using their approach.

Later, in [2] an Android application was developed and the experimental tests were performed on a Motorola Droid smartphone with a comparison to medical instruments (BioZ ECG and Nonin Onyx II model 9560BT ambulatory finger pulse oximeter). As a result, the validity of HR smartphone measurements was confirmed.

Scully et al. [6] developed a system for physiological parameter monitoring from optical recordings with a mobile phone. The videos were obtained by a Motorola Droid smartphone, and the PPG value was computed at each frame as the  $50 \times 50$  pixel average of the green channel region. The results for the heart rate were compared to the HP 78354A acquisition system using a standard 5-lead electrode configuration, and the respiration rate was compared with the metronome. In addition, the blue and red channels were used to detect the oxygen saturation and compared to the Masimo Radical SET<sup>TM</sup>. The high correlation of the results was reported as well.

It is well known that PPG measurements are very sensitive to patient and/or tissue movement artifacts. The automatic detection of such motion artifacts and their separation from good quality signal is a non-trivial task [16].

However, the above research works are based on testing the specific smartphone model for each case and do not refer to the problem of movement artifacts. On the other hand, as was already noted in [32], our tests show that the distribution of the pixels in either green or blue channels is not uniform for different smartphone models, such as HTC, iPhone4, Nokia, or Samsung. The only channel that has similar characteristics is the red one, while the rest can be used to distinguish a normal usage of the system from the abnormal one, when the finger is not located properly or there is no finger at all. Moreover, we noted that the red channel information remains similar even when the smartphone was used without LED, but in a well-illuminated environment.

Therefore, the aim of this research is to develop a method that would address these two problems. In this chapter, we describe a new method to measure the PPG waveform and calculate the pulse rate based on video obtained from a smartphone-based PPG acquisition system. The main emphasis is placed on the development of robust algorithms suitable for different smartphone models.

The rest of the chapter is organized as follows: in Section 5.2 we show a general system overview and the acquisition scheme, Section 5.3 deals with the correct usage assessment procedure, in Section 5.4 we explain the initial system calibration, the PPG evaluation algorithm and pulse computation procedure are described in Section 5.5, while in Section 5.6 the experimental results are presented and we conclude with Section 5.7.

## 5.2 System Work Overview

The proposed approach utilizes an image acquisition concept similar to the one of a pulse oximeter and PPG imaging. A subject covers with his fingertip a smartphone camera lens, trying to hold the finger steady and pressing without additional force (Figure 5.11). In this case the volumetric variation of blood changes the light absorption that passes through a finger. Such variation of light absorption is registered by a camera, and is used for PPG evaluation.

The measurements are performed continuously and for each new acquired frame the change of color values is computed. The feature of the proposed approach is that both reflection and transition modes of the system usage are

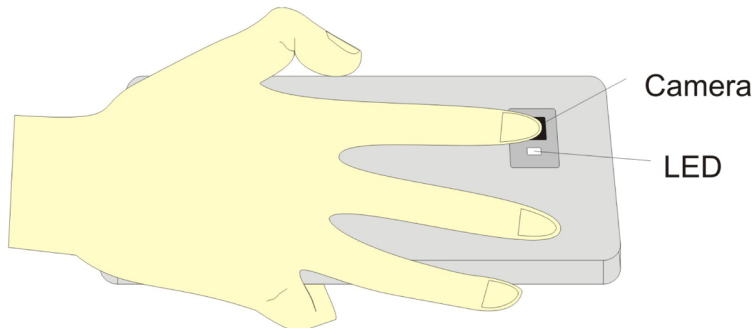


Figure 5.11 General video capturing scheme with a smartphone equipped by LED.

possible. Therefore, to evaluate pulsations it is possible to use smartphones with a LED as well as without it in the case of good lighting conditions.

After obtaining a new frame it is verified for correctness, as shown in the flow chart of the algorithm shown in Figure 5.12. Such verification procedure checks if the system is used in a proper mode: there is a finger in front of the camera and the illumination conditions are sufficient.

Then, there are two stages in the operation of the system: calibration and measurement. In the calibration stage the threshold value is established and the system parameters are updated while in the measurement stage the pulse rate is evaluated based on thresholding results and binary mask analysis. These two stages are explained in detail later in the appropriate sections of this chapter.

### **5.3 Assessment of Correct Use**

When health monitoring is performed in a clinical environment, the medical staff can supervise the whole procedure and detect when it goes wrong. However, when doing self-monitoring, only the person itself can control the correctness of this process. For example, the wrong position of the fingertip on the smartphone optical sensor or its absence, finger movement during the measurement or even changing the force with which fingertip presses the lens may cause wrong results and, as a result, the program gives false alarms or misses a dangerous situation. To prevent wrong health parameter measurement, the program automatically detects all cases of improper usage and instructs the person properly.

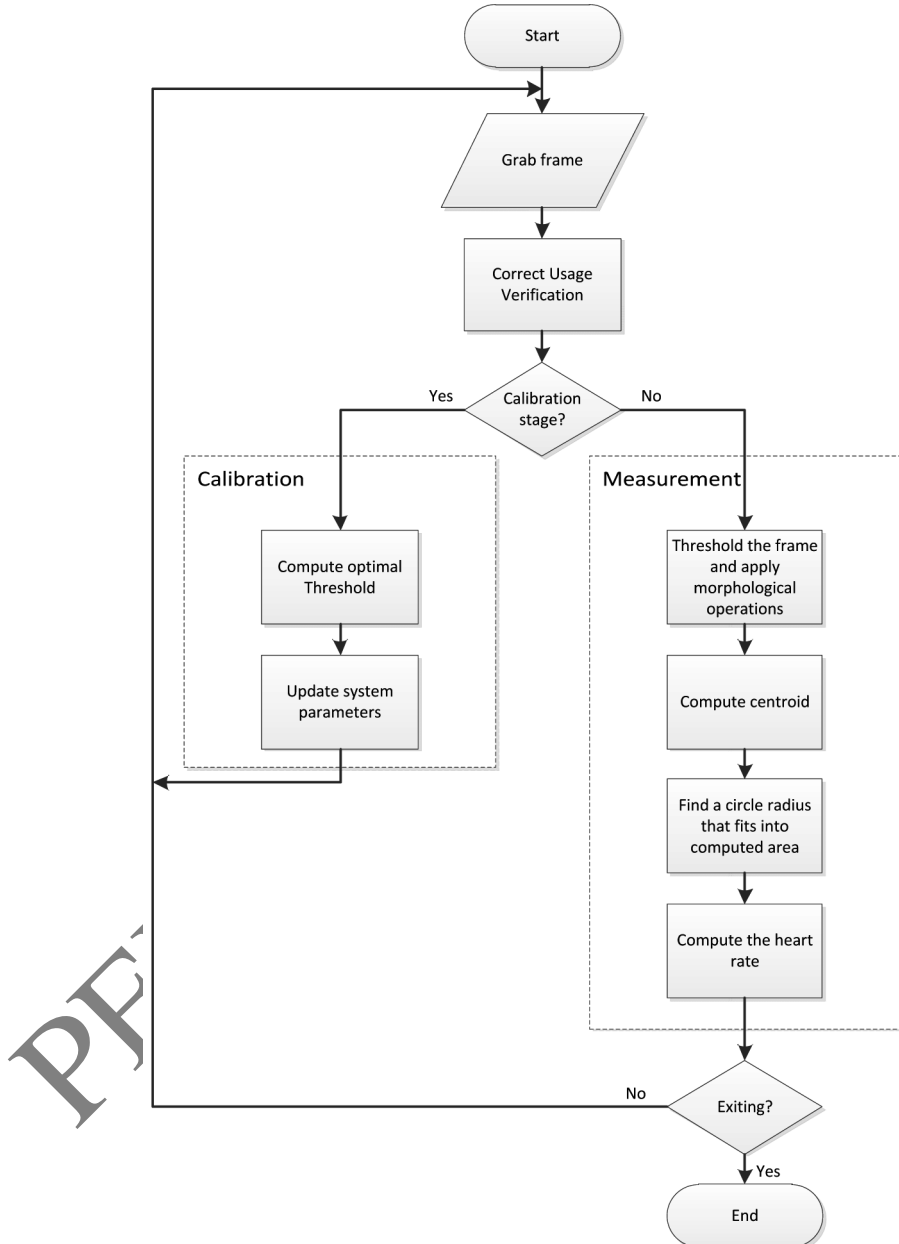


Figure 5.12 The PPG measurement algorithm which includes correct usage verification, calibration and measurement stages.

As it was stated previously, color saturation of the frames, acquired from different smartphones and in different illumination conditions, varies. Figure 5.13 shows the frames as well as the histograms of each color channel, obtained by HTC HD2, Nokia 5800, iPhone4, HTC HD2 without LED and Samsung Galaxy S i9000 smartphones, respectively.

It was also assessed experimentally that the values of the red and green color channels are much higher when the LED is used (i.e. in the light reflection mode) with respect to the case of light transmission. Thus, taking into account this value it is possible to automatically identify the usage mode and select appropriate system parameters.

In order to define the typical color model of the finger image a number of experiments with different smartphone models were carried out in different conditions. Some of the results obtained are illustrated in Figure 5.14.

The analysis of the results obtained (Figure 5.14) permits the following conclusions:

- when the LED is used:
  - pixel values in the green and blue color channels are concentrated in the lower half of their value range;
  - the red component values are concentrated in the top of the 0 to 255 range, and tend to the value 255.
- without using LED:
  - values of the green color channel are very low and are close the value 0;
  - the red component values in this case have no typical range. They vary for different phone models and depend on the patient finger's tissue and the amount of light that passes through it. However, they should be higher than some minimum value  $R_{NOLEDmin}$  as will be specified later. Otherwise, the small variation of the values, which happens when the illumination is not sufficient, makes further analysis impossible;
  - the values of the blue component vary depending on the smartphone model, but in general they tend to the value 0.

Hence, taking into account the above considerations, the state of the LED can be detected by the amount of green color in the frame.

In order to distinguish a proper usage of the system from an improper one, the following scheme was applied to each captured frame:

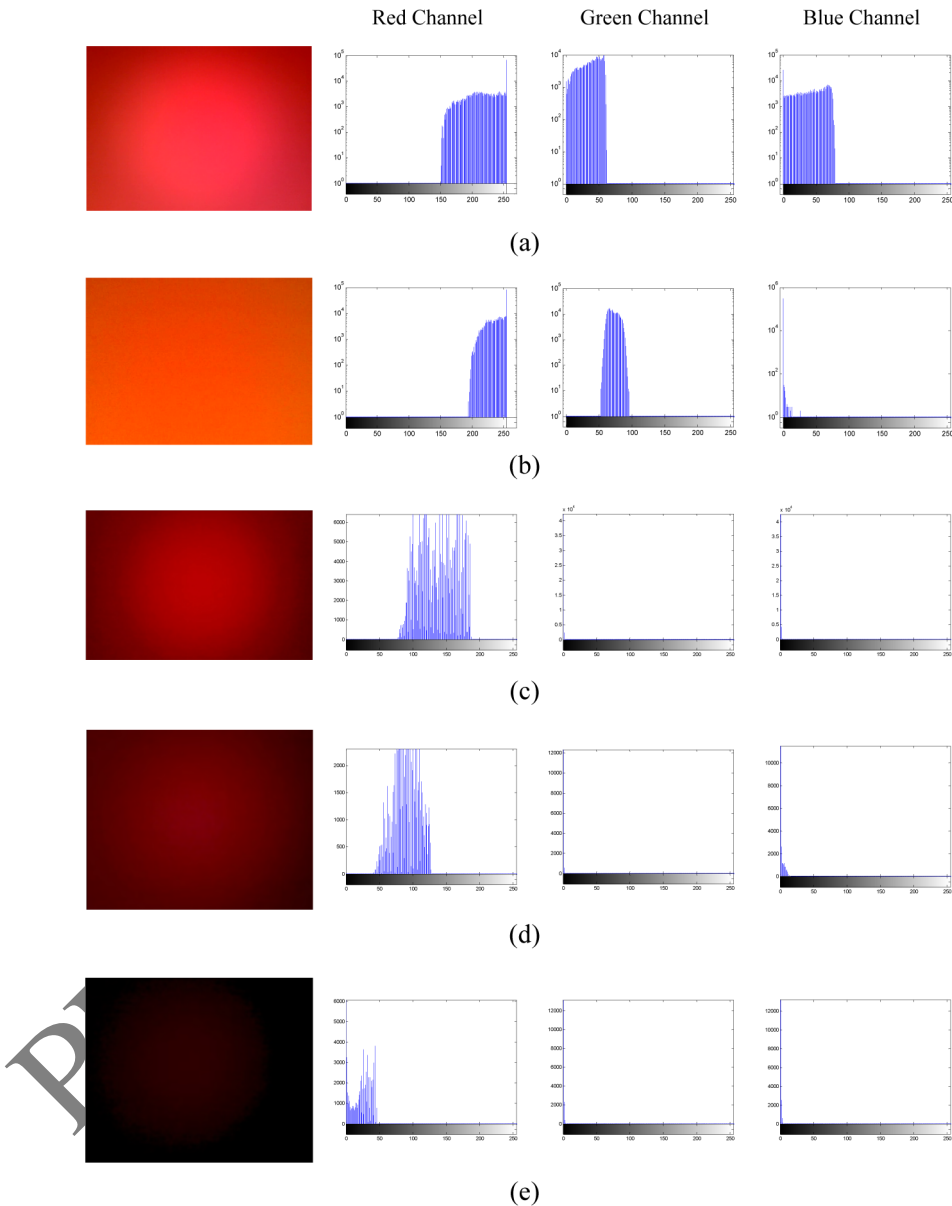


Figure 5.13 Acquired frames and their histograms of the red, green and blue channels for different smartphones and in different lighting conditions: (a) HTC HD2 with LED, (b) Nokia 5800 with LED, (c) iPhone4 with LED, (d) HTC HD2 without LED and (e) Samsung Galaxy S i9000 without LED.

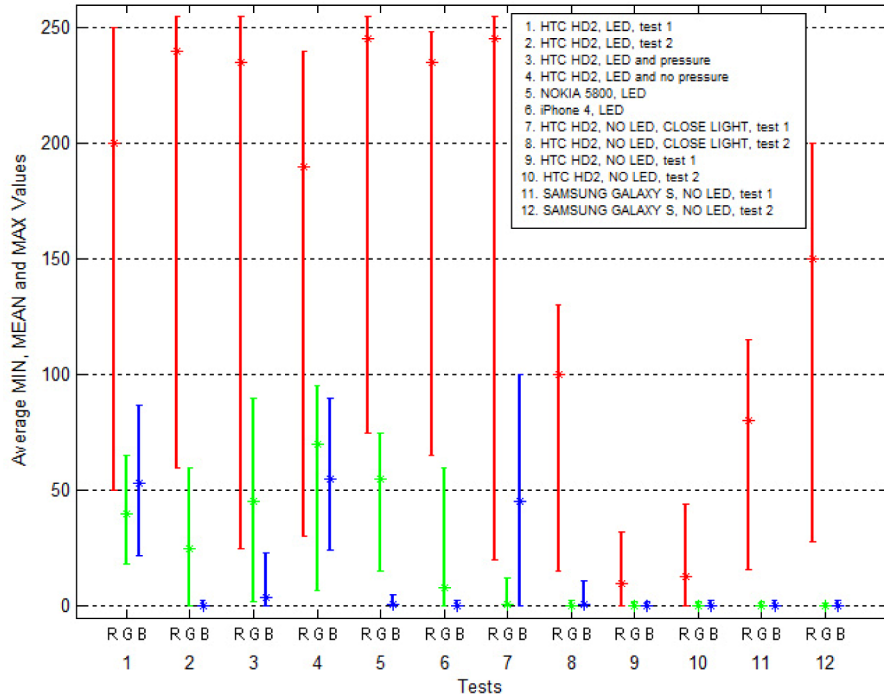


Figure 5.14 Distribution of the MIN, MEAN and MAX values of the pixels in RGB color space for videos captured using different smartphone cameras and under different lighting conditions.

% Color ranges when using LED:

$$\begin{aligned}
 & \text{mean}(G) + \sigma_G \geq G_{\text{LED}_{\min}} \quad \text{AND} \quad \% \text{ Green must not be small}, \\
 & \text{mean}(R) - \sigma_R \geq R_{\text{LED}_{\min}} \quad \text{AND} \quad \% \text{ Red should be mostly high}, \\
 & \text{mean}(G) + \sigma_G \geq G_{\max} \quad \text{AND} \quad \text{mean}(B) + \sigma_B < B_{\max} \quad \text{AND} \\
 & \quad \% \text{ Green and Blue should be mostly low} \\
 & \sigma_R, \sigma_G, \sigma_B < \sigma_{\max} \quad \% \text{ Values should not be distributed too much}
 \end{aligned} \tag{5.1}$$

OR

% Color ranges without LED use:

$$\text{mean}(G) + \sigma_G < G_{\text{NOLED}_{\max}} \quad \text{AND} \quad \% \text{ Green must be very small},$$

$$\begin{aligned}
 & \text{mean}(B) + \sigma_B < B_{\max} \quad \text{AND} \quad \% \text{ Blue should be mostly low,} \\
 & \text{mean}(R) > R_{\text{NOLED}_{\min}} \quad \text{AND} \quad \% \text{ Red must not be small} \\
 & \sigma_R, \sigma_G, \sigma_B < \sigma_{\max} \quad \% \text{ Values should not be distributed too much}
 \end{aligned} \tag{5.2}$$

where  $\text{mean}(R)$ ,  $\text{mean}(G)$  and  $\text{mean}(B)$  are the mean values of the red, green and blue components, respectively, computed for each captured frame,  $\sigma_R$ ,  $\sigma_G$ ,  $\sigma_B$  are the standard deviation values, computed for each frame and each color channel,  $G_{\text{LED}_{\min}}$  and  $R_{\text{LED}_{\min}}$  are the minimum values of the green and red channel, correspondingly, in the case the LED is used,  $G_{\max}$  and  $B_{\max}$  are the maximum values of the green and blue channels, respectively,  $\sigma_{\max}$  is the maximum standard deviation among all color channels,  $G_{\text{NOLED}_{\max}}$  is the maximum value of the green channel in the case the LED is not used,  $R_{\text{NOLED}_{\min}}$  is the minimum value of the red channel in the case the LED is not used.

The above scheme describes a proper color cluster in the RBG color space of the finger image. For the calibration stage the threshold values in (5.1) and (5.2) are defined based on the analysis of the preliminary experimental results. Thus, they are:  $G_{\text{LED}_{\min}} = 10$ ,  $R_{\text{LED}_{\min}} = 128$ ,  $G_{\max} = 128$ ,  $B_{\max} = 128$ ,  $\sigma_{\max} = 40$ ,  $G_{\text{NOLED}_{\max}} = 10$ ,  $R_{\text{NOLED}_{\min}} = 10$ , and are used to make sure that the finger is placed on the camera correctly. Such thresholds are valid for different models and used to define if initially the smartphone was used correctly. For the measurement phase, however, the threshold values are updated on the basis of the chromatic parameters of the acquired frames during the calibration stage. This is done to limit the possible color cluster to the characteristics of the current smartphone model, person's tissue and lighting conditions.

The validation step of the correct use is essential for further algorithm execution and quality assessment of the results, especially in the case of health monitoring systems. For the frames with no finger or with a finger in the wrong position, the color distribution in the channels does not fit defined rules, but it is spread out over the whole value range. Therefore, the proposed model allows considering only the case of finger presence, and, as a result, permits validating the correct use.

## 5.4 Initial System Calibration

As mentioned earlier, the system calibration step is used to adapt the system configuration to the particular smartphone camera and lighting conditions, as well as to the personal characteristics of the finger tissue (skin color, opacity, etc.). There are a few factors that must be taken into account to do that:

- (i) different smartphone models lead to different color saturation in the captured frames;
- (ii) different fingertip pressure force on the camera lens as well as different features of the tissue change the level of light absorption when it passes through the finger and, therefore, cause different color ratios;
- (iii) shifting the finger with respect to the camera lens creates motion artifacts and, as a result, causes wrong segmentation.

Considering the above cases it is clear that a fixed threshold value is not suitable. To compute the PPG signal it is possible to threshold the red components for each frame obtained and compute the number of pixels that surpass the threshold, as was proposed in [32]. The threshold  $T$  was established as 95% of the range between the  $\min$  and  $\max$  values during the first 5 s of system operation. That is:

$$T = \overline{\max}(I) - \frac{1}{20}(\overline{\max}(I) - \overline{\min}(I)) \quad (5.3)$$

where  $\overline{\max}(I)$  and  $\overline{\min}(I)$  are the mean maximum and minimum values, respectively, of the red component for the acquired frames during the first 5 s.

It was confirmed also that acquiring at least three full pulsations is enough, and the number of captured frames is suitable to perform statistical analysis. Such algorithm is reliable and works fine in the case the LED is used. However, if the system works without the LED the range between the  $\min$  and  $\max$  values is small and the number of computed pixels is not enough to make robust measurements. Moreover, it may occur that for some frames the maximum pixel value is lower than the established threshold, and the segmentation does not provide the expected result.

Hence, it was proposed to calculate the  $T$  as a mean of such values  $T_i$ , computed during the calibration step, at which the number of pixels in the corresponding thresholded image occupy more than  $\theta\%$  of the frame:

$$T = \text{mean}(T_i), T_i : \frac{\|\text{val}(P_i) \geq T_i\|}{\|P_i\|} = \theta\%, \quad i = 1, \dots, N, \quad (5.4)$$

where  $T_i$  is the computed threshold for frame  $i$ ,  $P_i$  is the array of red component pixels of the frame  $i$ ,  $\text{val}(P_i)$  is the value of each pixel in  $P_i$ ,  $\|\dots\|$  is the number of pixels in the array, and  $N$  is the number of frames for the calibration stage.

Since the finger is not fixed on the camera lens, it can shift during the measurement changing its position as well as its pressure on the lens. Therefore, it is necessary to ensure that the area, which surpasses the established threshold, always fits the image boundaries. Otherwise, the measurement would be incorrect. It was noted also that the pulsating dynamics (i.e. the difference between smallest and largest radii) is more for the pixels with high color values. It means that the final result is better if the threshold is high (closer to the max value of the pixels). In this work a value of  $\theta = 20$  is used.

Figure 5.15 shows examples of the thresholded image according to (5.4), captured from different smartphones and in different lighting conditions.

As can be seen from Figure 5.15a, the thresholded area contains some artifacts, caused by the close position of the LED and, as a result, high illumination of the pixels. The next section explains how to eliminate such artifacts and extract the proper PPG value.

## 5.5 PPG Evaluation Algorithm

As discussed previously, only the red component is suitable for PPG measurement since the figure shape remains similar for any smartphone model and any lighting conditions. Normally it has the shape of a paraboloid (Figure 5.16) with the maximum pixel value in the centre.

The shape of the thresholded binary mask depends on how the smartphone is used. Using a smartphone with a LED or specific finger position on the camera this shape can change. As was already mentioned, the mask in Figure 5.15a does not have a circular shape because the frame is acquired with the LED on, and some parts of the finger are better illuminated. Thus, a simple calculation of the number of pixels, as proposed in [32], cannot take into account the above factors.

To overcome this limit, we propose finding the circle that better fits the thresholded image, and use its radius as the PPG value. In particular, for each captured frame, we first calculate the coordinates  $C_x$  and  $C_y$  of a centroid of the binary mask as:

$$C_x = \frac{\sum_n x_n}{n}, \quad C_y = \frac{\sum_n y_n}{n}, \quad (5.5)$$

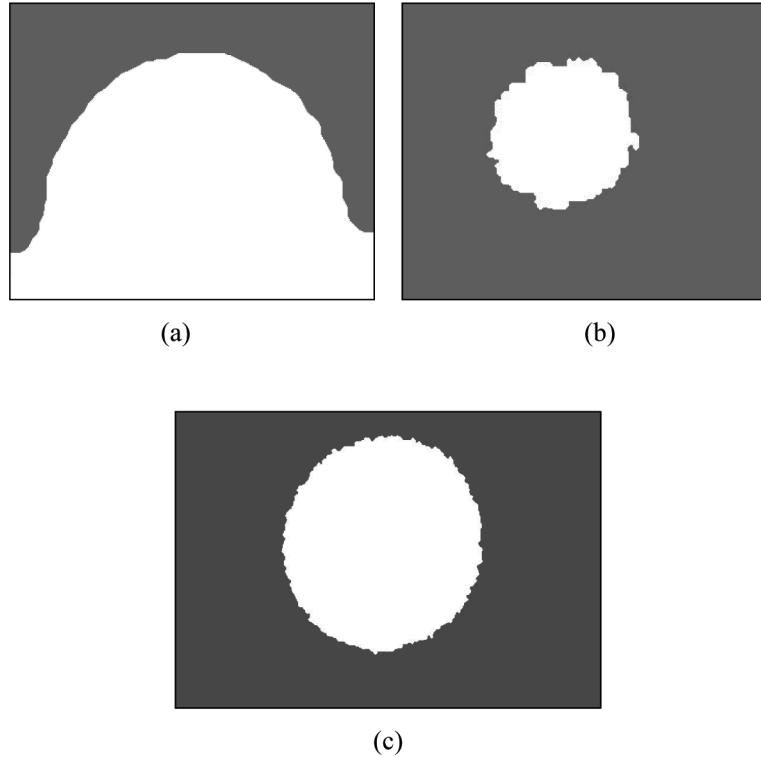


Figure 5.15 Computed masks that satisfy the threshold on the frames, captured (a) from HTC HD2 with LED, (b) HTC HD2 without LED, and (c) Samsung Galaxy S without LED.

where  $x_n$  and  $y_n$  are the coordinates of each pixel with a value 1 on a binary mask, and  $n$  is the total number of such values.

Then, the radius of the circle with the centre in the centroid is considered as a photoplethysmogram value (Figure 5.17).

Normally, the Hough transform can be applied to find the circles. However, such approach requires significant computational resources and also does not work well in the case of non-smooth boundaries. Since the computational complexity is important, it was proposed to compute the radius as follows (Figure 5.17):

1. find distance from the centroid to the boundary at positions  $0^\circ, 45^\circ, 90^\circ, 135^\circ, 180^\circ, 225^\circ, 270^\circ, 315^\circ$ ;
2. if the length exceeds the distance to the image boundaries, ignore this value;

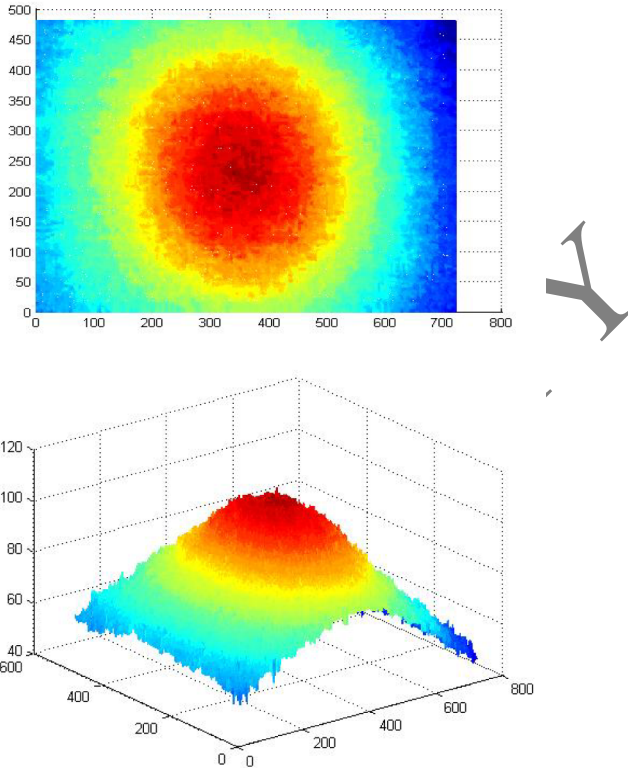


Figure 5.16 The pixels intensity and the surface of the red component for the frame captured from the Samsung Galaxy S smartphone.

3. find the mean value for all the remaining distances, and use it as the radius of a circle.

In this case, if the circle does not fit the image completely because of shifted centre, the radius will still be computed properly.

Computing the radius as described above for a sequence of captured frames gives a photoplethysmogram, where each cardiac cycle appears as a peak. Such waveform is generally referred to as the inverted PPG (Figure 5.18) [33], as the camera corresponds to the received rather than absorbed light intensity [24]. Thus, the final PPG signal is inverted vertically to be used for further processing.

Recovering the PR from such a PPG signal was achieved by passing the computed waveform with a 10s moving window and applying the Fourier

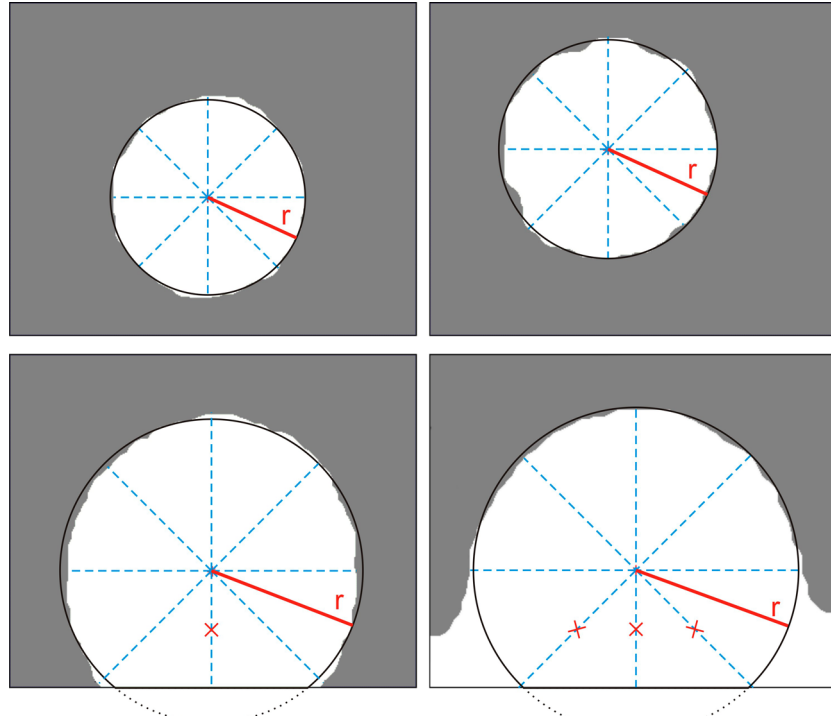


Figure 5.17 Computing the PPG value: white is a thresholded area; dashed lines are the distances from the centroid to the boundaries; crossed out lines are the lines that do not have a boundary on the image and should be skipped; solid bold lines are the radii, computed as average values of the above distances, solid lines – circles inscribed into the figures with radii  $r$ ; dotted lines are the parts of the circle that do not fit the picture.

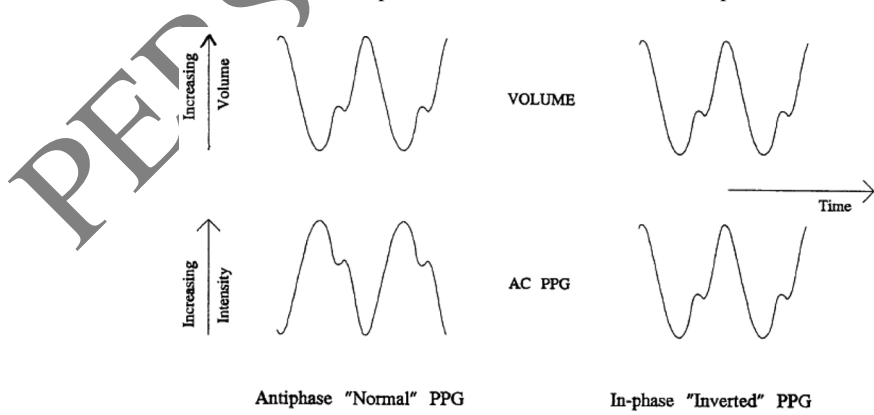


Figure 5.18 “Normal” and “inverted” PPG waveforms [33].

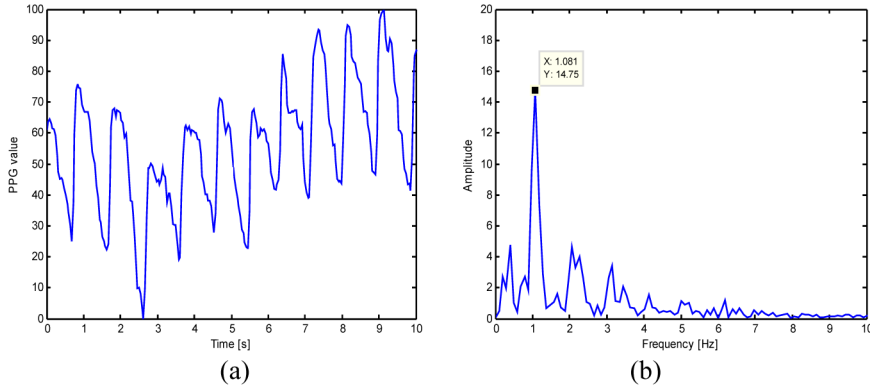


Figure 5.19 Measured PPG during a time interval of 10 s (a), and a corresponding Fourier spectrum. The evaluated value of PR is equal to 1.081 Hz (about 65 bpm) (b).

Table 5.1 Specification of the smartphones used for experiments.

Device name	Operating System	LED	Video resolution (pixels)	Frequency (fps)
HTC HD2	Windows Mobile 6.5	yes	352 × 288	25
Nokia 5800	Symbian OS v9.4	yes	640 × 480	29
Apple iPhone 4	iOS 4	yes	480 × 272	30
Samsung Galaxy S	Android OS, v2.3	no	720 × 480	30

transformation to each of the windows. The maximal peak on the spectrum near the frequency of 1Hz corresponds to the pulse rate frequency [29].

Figure 5.19 shows an example of computed PPG, inverted and normalized from 0 to 100, and the corresponding Fourier spectrum. The PPG signal itself is unfiltered. As it can be seen from Figure 5.19b, the evaluated PR is equal to 1.081 Hz and corresponds to about 65 beats per minute (bpm).

## 5.6 Experimental Results

The experimental tests were carried out using different smartphone models, in particular HTC HD2, iPhone4, Nokia 5800, Samsung Galaxy S i9000. Table 5.1 shows their specifications such as version of the operating system, presence of the LED, frames resolution and capturing frequency.

Videos from the smartphones were transferred to a computer, processed and compared to the data obtained from an oximeter. Further processing was done in Visual Studio C++ using the OpenCV library.

First, the system was tested to recognize the wrong usage cases. Therefore, a number of videos were captured with a finger positioned properly, and in a wrong mode. In particular, Figures 5.20a and 5.20b show examples and statistical values of the color components when the finger was positioned properly, while Figures 5.20c and 5.20d show the cases with no full contact between the finger and the phone camera. Other examples of wrong usage, when the finger did not cover the entire camera lens or even was not on the camera at all are shown in Figures 5.20e and 5.20f, respectively. In general, the proposed verification scheme allowed proper recognition of more than 98% wrong usage cases.

Then, to evaluate the accuracy of pulse measurements, the PPG waveforms were obtained simultaneously by the smartphone and the CMS50DL Finger Pulse Oximeter SPO<sub>2</sub> Monitor using two fingers of the left hand. Ten subjects participated in the test, going from 26 to 60 years of age. The PPG waveforms obtained by the smartphone were then inverted and normalized from 0 to 100 as explained before for further comparison.

As can be seen from Figure 5.21, which shows the two signals obtained by the smartphone and the oximeter in the normal subject state in the same time period, the peaks and the valleys correspond on both PPGs.

To prove the suitability and the correctness of the proposed method, the above test was repeated again just after squatting for 60 s. In this case the pulse rate changed because of the physical activity. As it is shown in Figure 5.22, the PPG evaluated by the smartphone shows more rapid pulsations and also corresponds to the one from oximeter.

Table 5.2 shows the summary of the tests where the mean PR and standard deviation value were computed for several measurements, performed with the HTC HD2 smartphone using LED and the CMS50DL Finger Pulse Oximeter SPO<sub>2</sub> Monitor at respective time periods. The signals were acquired for 60 s and the number of pulsations per minute was computed by applying the Fourier transform to a previous 10 s period.

Then, the mean and standard deviation values were computed. The same tests were performed using other smartphones and the results are shown in Figure 5.23. They confirm that the PPGs obtained from the smartphones are highly correlated to those obtained by a finger pulse oximeter and, therefore, can be used for PR measurements.

	Image	Statistical Data	Accepted
(a)		$\text{mean}(R) = 244.72,$ $\sigma_R = 16.65,$ $\text{mean}(G) = 26.51,$ $\sigma_G = 4.54,$ $\text{mean}(B) = 6.00,$ $\sigma_B = 9.52$	YES
(b)		$\text{mean}(R) = 144.35,$ $\sigma_R = 27.37,$ $\text{mean}(G) = 0.27,$ $\sigma_G = 0.46,$ $\text{mean}(B) = 0.25,$ $\sigma_B = 0.46$	YES
(c)		$\text{mean}(R) = 167.53,$ $\sigma_R = 50.08,$ $\text{mean}(G) = 49.14,$ $\sigma_G = 29.64,$ $\text{mean}(B) = 11.03,$ $\sigma_B = 15.79$	NO
(d)		$\text{mean}(R) = 242.34,$ $\sigma_R = 27.18,$ $\text{mean}(G) = 166.09,$ $\sigma_G = 47.01,$ $\text{mean}(B) = 114.41,$ $\sigma_B = 35.98$	NO
(e)		$\text{mean}(R) = 207.04,$ $\sigma_R = 90.07,$ $\text{mean}(G) = 205.01,$ $\sigma_G = 89.02,$ $\text{mean}(B) = 184.03,$ $\sigma_B = 97.12$	NO
(f)		$\text{mean}(R) = 134.04,$ $\sigma_R = 90.38,$ $\text{mean}(G) = 109.25,$ $\sigma_G = 80.13,$ $\text{mean}(B) = 77.11,$ $\sigma_B = 74.22$	NO

Figure 5.20 Accepted frames (a) and (b), frames recognized by the system as wrong because of not enough pressure of the finger (c), (d), wrong position on the camera (e), and missing of the contact between finger and camera (f).

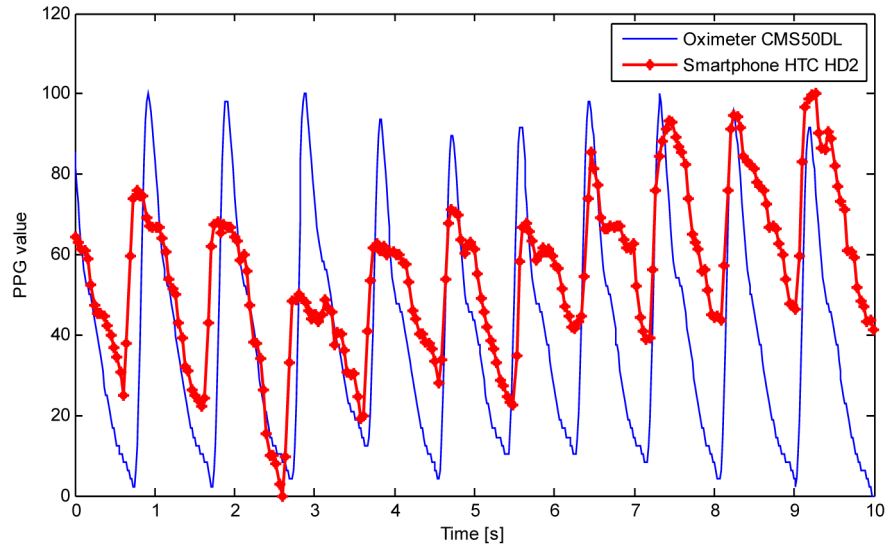


Figure 5.21 Comparison between the photoplethysmograms obtained by the smartphone HTC HD2 and the oximeter. The peaks and the valleys of both signals correspond.

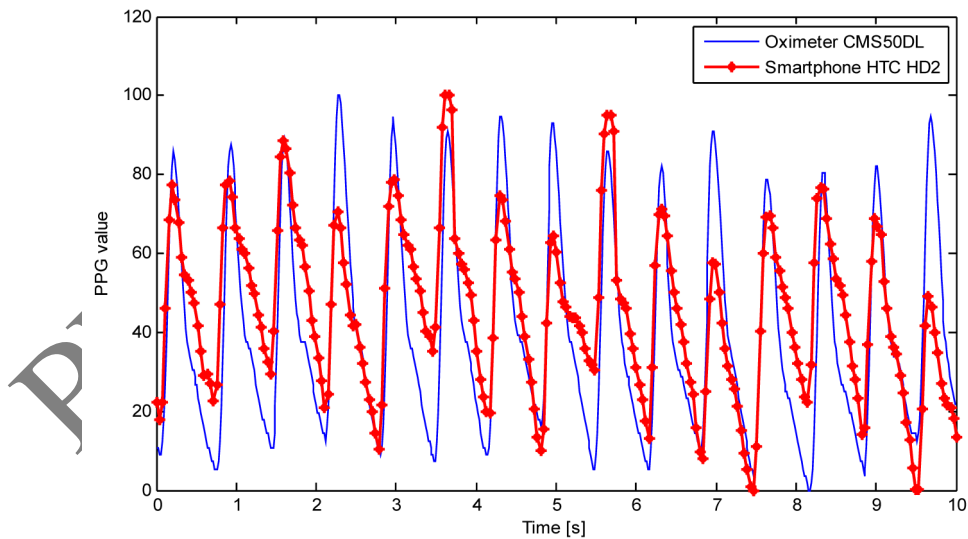


Figure 5.22 Comparison between the photoplethysmograms from the HTC HD2 smartphone and the oximeter after squatting for 60 s. Also in this case the peaks and the valleys of both signals are highly correlated.

Table 5.2 Comparison between the PR evaluated from the HTC HD2 using LED and the CMS50DL Finger Pulse Oximeter SPO2 Monitor.

Test No.	Mean PR from smartphone (bpm)	Mean PR from oximeter (bpm)	Error (%)
Video 1, before squatting	61.46 ± 1.48	62.07 ± 1.34	0.98
Video 2, after squatting	90.15 ± 4.6	91.58 ± 3.29	1.56
Video 3, before squatting	79.42 ± 3.23	79.80 ± 3.14	0.48
Video 4, after squatting	98.86 ± 12.15	97.79 ± 11.17	1.09
<b>Average Error</b>			<b>1.03</b>

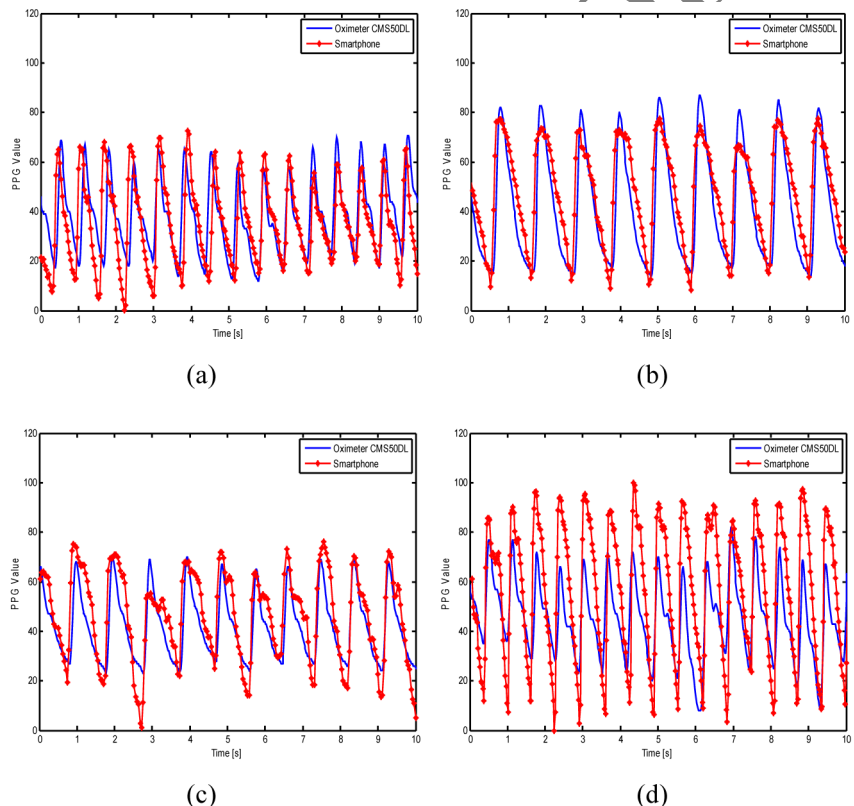


Figure 5.23 PPG waveforms obtained from (a) Nokia 5800 with the LED enabled, (b) iPhone4 with LED, (c) HTC HD2 without LED, (d) Samsung Galaxy S i9000 without LED, and the corresponding waveform, acquired from a CMS50DL Finger Pulse Oximeter SPO2 Monitor.

## 5.7 Conclusions

This chapter is devoted to the photoplethysmogram measurement by means of a smartphone and integrated camera. Prior work has reported the possibility of smartphone usage for pulse rate measurement. The successful application of the green color component for PPG signal computing was reported.

However, such reports involved a limited number of smartphones and further research has shown that the typical color range varies from model to model, this has been demonstrated in this chapter. In particular, it has been shown that only the red channel has similar characteristics for different models of smartphones while the green and blue may vary dramatically. Although the last two components do not have a fixed color range, they can be used to detect a wrong usage of the system.

The proposed PPG evaluation method is suitable to work in both reflection and transmission modes, and allows evaluating the PPG when the LED is not used. The appropriate algorithms for the correct usage verification procedure and the initial system calibration were proposed and tested. In addition, an improved PPG value calculation algorithm was proposed.

The experimental tests were carried out with smartphone models such as the HTC HD2, iPhone4, Samsung Galaxy S i9000 and Nokia 5800. Devices, equipped with LED were tested in two modes: when the LED was enabled and disabled. A total of 10 persons aged between 26 and 60 years took part in the experiments. The obtained results were compared to the CMS50DL Finger Pulse Oximeter SPO<sub>2</sub> Monitor. The pulse rates obtained as well as the signals themselves were comparable between all the devices. Thus, it confirms the correctness and reliability of the proposed PPG calculation technique with respect to medical pulse measurement instruments.

In future work it would be interesting to evaluate more parameters from the obtained PPG signal, as well as test it on wider set of smartphones and patients.

## References

- [1] D.J. Terbisan, B.A. Dolezal, and C. Albano. Validity of seven commercially available heart rate monitors. *Measurement in Physical Education and Exercise Science*, 6(4):243–247, 2009.
- [2] M.J. Gregoski, M. Mueller, A. Vertegel, et al. Development and validation of a smartphone heart rate acquisition application for health promotion and wellness telehealth applications. *International Journal of Telemedicine and Applications*, doi: 10.1155/2012/696324, 2012.

- [3] A. Kumar. ECG – simplified, *LifeHugger*, November 2010.
- [4] T.G. Pickering. White coat hypertension. *Current Opinion in Nephrology and Hypertension*, 5(2):192–198, March 1996.
- [5] A. Smith and T. Ferriss. Home health monitoring may significantly improve blood pressure control. *Kaiser Permanente Study Finds*, May 2010.
- [6] C.G. Scully, J. Lee, J. Meyer, A.M. Gorbach, D. Granquist-Fraser, Y. Mendelson, and H. Chon Ki. Physiological parameter monitoring from optical recordings with a mobile phone. *IEEE Transactions on Biomedical Engineering*, 59(2):303–306, 2012.
- [7] V. Gay and P. Leijdekkers. A health monitoring system using smart phones and wearable sensors. *International Journal of ARM*, 8(2):29–35, 2007.
- [8] M.E. Ernst and G.R. Bergus. Ambulatory blood pressure monitoring. *Southern Medical Journal*, 96(6):563–568, June 2003.
- [9] Operations Manual 90207-80/90217-1HABP Monitors, 070-0715-00 Rev. B, Spacelabs Medical, Inc.
- [10] A. Shennan, A. Halligan, M. Gupta, D. Taylor, and M. de Swiet. Oscillometric blood pressure measurements in severe per-eclampsia: Validation of the SpaceLabs 90207. *BJOG: An International Journal of Obstetrics & Gynaecology*, 103(7):171–173, 1996.
- [11] C.W. Belsha, T.G. Wells, H.B. Rice, W.A. Neaville, and P.L. Berry. Accuracy of the SpaceLabs 90207 ambulatory blood pressure monitor in children and adolescents. *Blood Pressure Monitoring*, 1:127–133, 1996.
- [12] P. Iqbal, M.D. Fotherby, and J.F. Potter. Validation of the SpaceLabs 90207 automatic non-invasive blood pressure monitor in elderly subjects. *Blood Pressure Monitoring*, 1:367–373, 1996.
- [13] Association for the Advancement of Medical Instrumentation, <http://www.aami.org>.
- [14] American Heart Association, Inc., <http://www.heart.org>.
- [15] British Hypertension Society, <http://www.bhsoc.org>.
- [16] J. Allen. Photoplethysmography and its application in clinical physiological measurement. *Physiological Measurement*, 28:R1–R39, 2007.
- [17] E. Jonathan and M. Leahy. Investigating a smartphone imaging unit for photoplethysmography, *Physiological Measurement*, 31(11):N79–N83, November 2010.
- [18] D. Damianou. The wavelength dependence of the photoplethysmogram and its implication to pulse oximetry. Doctor of Philosophy Thesis, University of Nottingham, October 1995.
- [19] A. Reisner, P. Shaltis, D. McCombie, and H. Asada. Utility of the photoplethysmogram in circulatory monitoring. *Anesthesiology*, 108(5):950–958, May 2008.
- [20] P. Leonard, N. Grubb, P. Addison, D. Clifton, and J. Watson. An algorithm for the detection of individual breaths from the pulse oximeter waveform. *Journal of Clinical Monitoring and Computing*, 18(5–6):309–312, December 2004.
- [21] S. Linder, S. Wendelken, E. Wei, and S. McGrath. Using the morphology of photoplethysmogram peaks to detect changes in posture. *Journal of Clinical Monitoring and Computing*, 20(3):151–158, June 2006.
- [22] U. Rubins. Finger and ear photoplethysmogram waveform analysis by fitting with Gaussians. *Medical and Biological Engineering and Computing*, 46(12):1271–1276, December 2008.

- [23] Jia Zheng and Sijung Hu. The preliminary investigation of imaging photoplethysmographic system. *Journal of Physics: Conference Series*, 85, doi:10.1088/1742-6596/85/1/012031, 2007.
- [24] Jia Zheng, Sijung Hu, V. Azorin-Peris, Angelos Echiadis, V. Chouliaras, and R. Summers. Remote simultaneous dual wavelength imaging photoplethysmography: A further step towards 3-D mapping of skin blood microcirculation. *Multimodal Biomedical Imaging III, Proc. of SPIE*, 6850, 68500S-1, 2008.
- [25] iHealth Blood Pressure Monitoring System, Medisana AG, <http://ihealth.medisana.com/en/index.php>.
- [26] D.L. Carnì, G. Fortino, R. Gravina, D. Grimaldi, A. Guerrieri, and F. Lamonaca. Continuous, real-time monitoring of assisted livings through wireless body sensor networks. In *Proceedings of the IEEE International Conference Intelligent Data Acquisition and Advanced Computing Systems IDAACS'2011*, pp. 872–877, September 2011.
- [27] M.N. Kamel Boulos, C. Tavares et al., How smartphones are changing the face of mobile and participatory healthcare: An overview, with example from eCAALYX. *BioMedical Engineering OnLine*, 10(24), 2011.
- [28] P. Pelegris, K. Banitsas, T. Orbach, and K. Marias. A novel method to detect heart beat rate using a mobile phone. In *Proceedings of 32nd IEEE Annual International Conference on Merging Medical Humanism and Technology*, pp. 5488–5491, 2010.
- [29] W. Verkruyse, L.O. Svaasand, and J.S. Nelson. Remote plethysmographic imaging using ambient light. *Optics Express*, 16(26):21434–21445, 2008.
- [30] S.C. Millasseau, J.M. Ritter, K. Takazawa, and P.J. Chowienczyk. Contour analysis of the photoplethysmographic pulse measured at the finger. *Journal of Hypertension*, 24(8):1449–1456, 2006.
- [31] E. Jonathan and M.J. Leahy. Cellular phone-based photoplethysmographic imaging. *Journal on Biophotonics*, 4(5):293–296, 2011.
- [32] D. Grimaldi, Yu. Kurylyak, F. Lamonaca, and A. Nastro. Photoplethysmography detection by smartphone's videocamera. In *Proceedings of IEEE International Conference Intelligent Data Acquisition and Advanced Computing Systems IDAACS'2011*, pp. 488–491, September 2011.
- [33] J. Nijboer, J. Dorlas, and H. Mahieu. Photoelectric plethysmography: Some fundamental aspects of the reflection and transmission method. *Clinical Physics and Physiological Measurement*, 2(3):205–215, 1981.